2015

Finite-size scaling, dynamic fluctuations, and hyperscaling relation in the Kuramoto model

Hyunsuk Hong
Department of Physics, Research Institute of Physics and Chemistry, Chonbuk National University

Hugues Chaté
Service de Physique de l'Etat Condensé, CEA-Saclay, CNRS UMR 3680, zhanghj@hkbu.edu.hk

Lei-Han Tang
Department of Physics, Hong Kong Baptist University, lhtang@hkbu.edu.hk

Hyunggyu Park
School of Physics and QUC, Korea Institute for Advanced Study, liangchao512@163.com

This document is the authors' final version of the published article.

Citation

Finite-size scaling, dynamic fluctuations, and hyperscaling relation in the Kuramoto model

Hyunsuk Hong,[1] Hugues Chaté,[2,3] Lei-Han Tang,[4,3] and Hyunggyu Park[5]

[1]*Department of Physics and Research Institute of Physics and Chemistry, Chonbuk National University, Jeonju 561-756, Korea*
[2]*Service de Physique de l'Etat Condensé, CEA-Saclay, CNRS UMR 3680, 91191 Gif-sur-Yvette, France*
[3]*Beijing Computational Science Research Center, Beijing 100084, China*
[4]*Department of Physics, Hong Kong Baptist University, Kowloon Tong, Hong Kong SAR, China*
[5]*School of Physics and QUC, Korea Institute for Advanced Study, Seoul 130-722, Korea*

We revisit the Kuramoto model to explore the finite-size scaling (FSS) of the order parameter and its dynamic fluctuations near the onset of the synchronization transition, paying particular attention to effects induced by the randomness of the intrinsic frequencies of oscillators. For a population of size N, we study two ways of sampling the intrinsic frequencies according to the *same* given unimodal distribution $g(\omega)$. In the "*random*" case, frequencies are generated independently in accordance with $g(\omega)$, which gives rise to oscillator number fluctuation within any given frequency interval. In the "*regular*" case, the N frequencies are generated in a deterministic manner that minimizes the oscillator number fluctuations, leading to quasiuniformly spaced frequencies in the population. We find that the two samplings yield substantially different finite-size properties with clearly distinct scaling exponents. Moreover, the hyperscaling relation between the order parameter and its fluctuations is valid in the regular case, but it is violated in the random case. In this last case, a self-consistent mean-field theory that completely ignores dynamic fluctuations correctly predicts the FSS exponent of the order parameter but not its critical amplitude.

I. INTRODUCTION

We revisit the Kuramoto model [1] to investigate the phase order parameter and its dynamic fluctuations near the onset of the synchronization transition. In particular, we focus on their critical finite-size scaling (FSS) behavior. Even though the Kuramoto model and its extended versions have been widely studied [2,3], some issues persist, particularly those regarding the above points. In the few existing studies [4,5], the critical properties near the transition point have only been partially resolved, which prompted the present work.

FSS is particularly important for data analysis, since real systems are always finite, and particularly so in many experimental systems, biological or not [6]. Recently, the FSS of the synchronization order parameter in the Kuramoto model and several extended versions on complex networks has been investigated. An unusual FSS exponent $\bar{\nu} = \frac{5}{2}$ has been found [7–9]. This value was obtained in the classic case, hereafter referred to as the *random distribution*, where the individual frequencies of oscillators are sampled independently according to a given unimodal distribution $g(\omega)$. In such a situation, oscillator frequencies can be arbitrarily close to each other even in a finite population. Interestingly, when the oscillator density fluctuation along the frequency axis is suppressed in a population with *regular distribution*, a very different FSS exponent $\bar{\nu} = \frac{5}{4}$ is obtained. Here we present details of our numerical study that led to this previously reported value [10,11].

Dynamic fluctuations of the order parameter in the Kuramoto model are another long-standing problem [3,12]. In the perturbation theory developed by Daido [4], it is claimed that they scale differently when approaching the synchronization threshold from above and from below, with the scaling exponent $\gamma = \frac{1}{4}$ in the supercritical region and $\gamma' = 1$ in the subcritical region. This result is quite surprising by itself, in the sense that conventional scaling theory predicts identical scaling behavior on either side of the transition. Note that Daido used the regular frequency distribution in numerical investigations as well as in his perturbation theory [4].

In this paper, we report extensive numerical results on the FSS of the order parameter and its dynamic fluctuation in the random and regular realizations of the intrinsic frequency distribution. The FSS exponent in the regular case is estimated numerically as $\bar{\nu} \simeq \frac{5}{4}$, which is half the value of its random counterpart. In contrast to Daido's predictions, we find that dynamic fluctuations scale with the same exponent $\gamma = \gamma'$ on both sides of the transition. Interestingly, our data support $\gamma \simeq \gamma' \simeq 1$ for the random frequency distribution and $\gamma \simeq \gamma' \simeq \frac{1}{4}$ for the regular case. Given the order-parameter exponent $\beta = \frac{1}{2}$, the hyperscaling relation $\gamma = \bar{\nu} - 2\beta$ is thus violated in the random case, but it is obeyed in the regular case. We finally briefly discuss the implications of our observations on the ordering process and dynamic response in the Kuramoto model.

The paper is organized as follows. In Sec. II, we introduce the Kuramoto model and present the two types of frequency realizations that we consider in this paper. In Sec. III, we investigate the FSS of the order parameter and its dynamic fluctuations with the random frequency distribution, and we discuss the validity of the hyperscaling relation in the model. In Sec. IV, we repeat the investigation and analysis with the regular distribution. We summarize and discuss the results in Sec. V. Appendix presents the mean-field approximation to the FSS in the case of the random frequency distribution.

II. THE KURAMOTO MODEL

The Kuramoto model [1] consists in a finite population of N globally coupled phase oscillators governed by

$$\frac{d\phi_j}{dt} = \omega_j - \frac{K}{N}\sum_{k=1}^{N}\sin(\phi_j - \phi_k), \quad j = 1,\ldots,N. \quad (2.1)$$

Here ϕ_j is the phase of the jth oscillator, and ω_j is its intrinsic frequency. A *given realization* of the Kuramoto model corresponds to a particular choice of the N intrinsic frequencies $\{\omega_j\}$. In this paper, we shall assume that the number density of these frequencies on the real axis follows, on average, the normal distribution $g(\omega) = (1/\sqrt{2\pi})e^{-\omega^2/2}$. The coupling strength K is positive ($K > 0$).

Phase synchronization is conveniently described by the complex order parameter defined as [1]

$$Z(t) \equiv \Delta e^{i\theta} = \frac{1}{N}\sum_{j=1}^{N} e^{i\phi_j}, \qquad (2.2)$$

where a nonzero (positive) value of Δ in the asymptotic $N \to \infty$ limit implies the emergence of phase synchronization, and θ is the phase of the global order parameter. With this definition, Eq. (2.1) is rewritten as

$$\dot{\phi}_j = \omega_j - K\Delta\sin(\phi_j - \theta), \qquad (2.3)$$

where both Δ and θ are dynamic variables defined by Eq. (2.2). In the limit $N \to \infty$, the model exhibits a continuous symmetry-breaking transition at $K = K_c = 2/[\pi g(0)] = \sqrt{8/\pi}$ [1]. In this limit, the phase order parameter is strictly zero on the subcritical side ($K < K_c$), while on the supercritical side ($K > K_c$),

$$\Delta \sim (K - K_c)^\beta \quad \text{with} \quad \beta = \tfrac{1}{2}. \qquad (2.4)$$

This result holds for any unimodal and symmetric $g(\omega)$.

For a finite population of oscillators, $\Delta(t)$ exhibits both dynamic and sample-to-sample fluctuations whose scaling with N is the main focus of this work. The sample-to-sample fluctuations arise from the randomly drawn oscillator frequencies from the distribution $g(\omega)$. Consequently, the spacing between neighboring frequencies on the real axis is Poissonian in any given realization. It turns out that this quenched noise and the nonlinear dynamic fluctuations are intimately related to each other in the sense that, when the former is removed, a very different set of FSS exponents are obtained. The two types of oscillator frequency distributions are discussed in Secs. III and IV, respectively.

III. RANDOM FREQUENCY DISTRIBUTION

In this section, we consider the realizations (samples) of frequency sets $\{\omega_j\}$ by randomly and independently drawing frequencies from the Gaussian distribution $g(\omega)$. We measure the phase order parameter and its dynamic fluctuation for each sample and average over many samples. In practice, we numerically integrate Eq. (2.3), for system sizes up to $N = 12\,800$, using Heun's method [13] with a discrete time step $\delta t = 0.01$, up to a total of 2×10^5 time steps. We start with random initial values of $\{\phi_j(0)\}$ and average the data over time after the first 10^5 steps to avoid any transient behavior, and we also average over 10^2–10^3 different samples of $\{\omega_j\}$ and $\{\phi_j(0)\}$. At $K = K_c$, we perform numerical integration for larger systems up to $N = 204\,800$ with twice as many realizations.

A. Finite-size scaling of the order parameter

In analogy with equilibrium critical phenomena, we expect the order parameter in the critical region to satisfy the FSS [14],

$$\Delta(K,N) = N^{-\beta/\bar{\nu}} f(\epsilon N^{1/\bar{\nu}}), \qquad (3.1)$$

where $\epsilon = K - K_c$ and the scaling function $f(x)$ is a monotonically increasing function with the following asymptotic properties:

$$f(x) \sim \begin{cases} x^\beta, & x \gg 1, \\ (-x)^{\beta - \bar{\nu}/2}, & x \ll -1. \end{cases} \qquad (3.2)$$

The exponent $\bar{\nu}$ is known as the FSS exponent. For large N, this scaling ansatz reproduces Eq. (2.4) on the supercritical side, and it yields $\Delta \sim N^{-\beta/\bar{\nu}}$ at the transition and $\Delta \sim N^{-\frac{1}{2}}$ in the subcritical regime, respectively.

In the usual mean-field treatment of the Kuramoto model, the entrained state is established by solving Eq. (2.3) at a constant Δ and θ (dynamic fluctuations are ignored): Oscillators with $|\omega_j| < K\Delta$ get into an entrained (locked) state, reaching a fixed angle. On the other hand, the oscillators with $|\omega_j| > K\Delta$ perform periodic motion with modified frequencies. With this, the self-consistent equation for Δ from Eq. (2.2) can be written as

$$\Delta = \int_{-K\Delta}^{K\Delta} d\omega\, g(\omega)\sqrt{1 - (\omega/K\Delta)^2} \qquad (3.3)$$

in the $N \to \infty$ limit. Equation (3.3) has a nontrivial solution ($\Delta > 0$) for $K > K_c = 2/[\pi g(0)]$.

For a finite-size system, the right-hand side of Eq. (3.3) is replaced with

$$\Delta = \Psi(K\Delta) \equiv \frac{1}{N}\sum_{j, |\omega_j| < K\Delta} \sqrt{1 - (\omega_j/K\Delta)^2}, \qquad (3.4)$$

which contains a sample-dependent correction $\delta\Psi \equiv \Psi - [\Psi] \propto \sqrt{N_s}/N$ [8]. Here N_s is the number of (entrained) oscillators in the frequency interval $(-K\Delta, K\Delta)$, and $[\cdot]$ denotes sample average. As was shown previously in Refs. [8,10] and is explained in detail in Appendix, for K close to K_c, Eq. (3.4) admits a scaling solution of the form (3.1) with the exponents

$$\beta = \tfrac{1}{2} \quad \text{and} \quad \bar{\nu} = \tfrac{5}{2}. \qquad (3.5)$$

The scaling function $f(x)$, however, has significant sample-to-sample fluctuations.

The exponent value $\beta = \frac{1}{2}$ is typical of various equilibrium mean-field models described by the so-called ϕ^4 theory. However, the FSS exponent value of $\bar{\nu} = \frac{5}{2}$ is quite unusual and implies much stronger fluctuations than that in ordinary models with the conventional value $\bar{\nu} = 2$. This remarkable result has been confirmed by extensive numerical simulations [7,8] and the straightforward extension to the Kuramoto model on various sparse random networks in [9,11,14].

B. Dynamic fluctuations

Now, we consider the dynamic (temporal) fluctuations of the order parameter by measuring the quantity [15]

$$\chi(K,N) \equiv N[\langle(\Delta - \langle\Delta\rangle)^2\rangle] = N[\langle\Delta^2\rangle - \langle\Delta\rangle^2], \qquad (3.6)$$

where $\langle \cdot \rangle$ denotes the time average in the steady state of a given sample and $[\cdot]$ denotes the sample average, respectively.

For $K < K_c$, we expect from simple power counting that $\chi \sim O(1)$, because $\Delta \sim N^{-\frac{1}{2}}$. For $K > K_c$, the order parameter becomes $O(1)$, but these $O(1)$ terms cancel out each other exactly and the next-order terms proportional to $N^{-\frac{1}{2}}$ contribute. Again, χ becomes $O(1)$. However, at $K = K_c$, strong critical FSS occurs since $\Delta \sim N^{-\beta/\bar{\nu}} = N^{-\frac{1}{5}}$, and one can expect that χ will diverge in the $N \to \infty$ limit. Summing up, the critical behavior of χ near the transition may be expressed, in the $N \to \infty$ limit, as

$$\chi \sim \begin{cases} \epsilon^{-\gamma}, & \epsilon > 0, \\ (-\epsilon)^{-\gamma'}, & \epsilon < 0. \end{cases} \tag{3.7}$$

The two exponents γ and γ' describe the divergence of χ in the supercritical ($\epsilon > 0$) and subcritical ($\epsilon < 0$) regions, respectively.

For homogeneous systems, scaling in the critical region is controlled by a single fixed point in the renormalization-group (RG) sense, and hence $\gamma = \gamma'$. The corresponding FSS takes the form

$$\chi(\epsilon, N) = N^{\gamma/\bar{\nu}} h(\epsilon N^{1/\bar{\nu}}), \tag{3.8}$$

irrespective of the side of the transition, and the scaling function $h(x)$ has the limiting behavior

$$h(x) \sim \begin{cases} \text{const}, & x = 0, \\ x^{-\gamma}, & x \gg 1, \\ (-x)^{-\gamma}, & x \ll -1. \end{cases} \tag{3.9}$$

In this context, the Kuramoto model is somewhat special in that each oscillator has its own intrinsic frequency and the effect of the mean field is different on different oscillators. Therefore, the usual RG argument with only a few relevant variables may not apply, and one should entertain the possibility that $\gamma \neq \gamma'$. In such a situation, the FSS exponent $\bar{\nu}$ should also be different on the two sides of the transition, so that the ratio relation $\gamma/\bar{\nu} = \gamma'/\bar{\nu}'$ is satisfied, in order to maintain the continuity of χ at $\epsilon = 0$. Indeed, through perturbative calculation, Daido [4] obtained $\gamma = \frac{1}{4}$ and $\gamma' = 1$.

We have carried out extensive numerical simulations to obtain accurate estimates of γ and γ' as well as other FSS exponents. Figure 1 shows numerical data for χ versus ϵ for various system sizes N. As expected, finite-size effects become huge near the transition point. We observe two important features of the finite-size effects: First, the peak position at $K = K_{\max}$ is always on the subcritical side ($\epsilon < 0$) and approaches the bulk critical point ($\epsilon = 0$) as N increases. Second, the peak height $\chi_{\max}$ grows rapidly with N. By analyzing the data for the peak position and height, we estimate γ' and $\bar{\nu}'$ in the subcritical side, using the conventional FSS ansatz

$$\chi_{\max} \sim N^{\gamma'/\bar{\nu}'}, \quad \delta K_{\max} \sim N^{-1/\bar{\nu}'} \tag{3.10}$$

with $\delta K_{\max} \equiv |K_{\max} - K_c|$. As shown in Figs. 2(a) and 2(b), both quantities exhibit power-law scaling with the exponent values

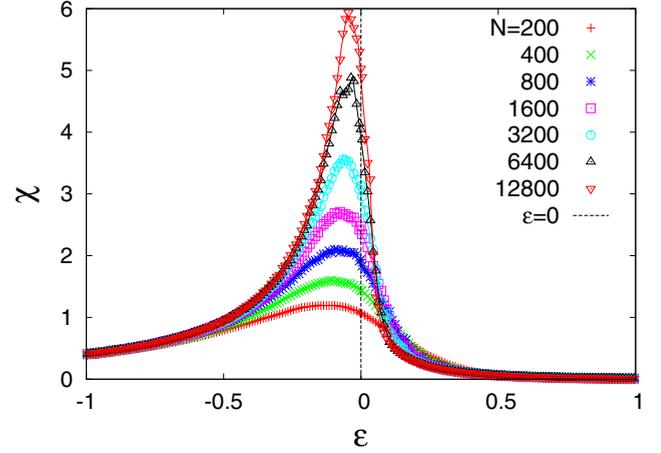$$\gamma'/\bar{\nu}' = 0.40(1), \quad 1/\bar{\nu}' = 0.33(8). \tag{3.11}$$

FIG. 1. (Color online) Dynamic fluctuation χ against $\epsilon = K - K_c$ for various system size N, with $K_c = \sqrt{8/\pi}$. The data have been obtained from the average over 100–1000 samples with different sets of $\{\omega_j\}$ and initial phases $\{\phi_j(0)\}$. Statistical errors are represented by symbol sizes.
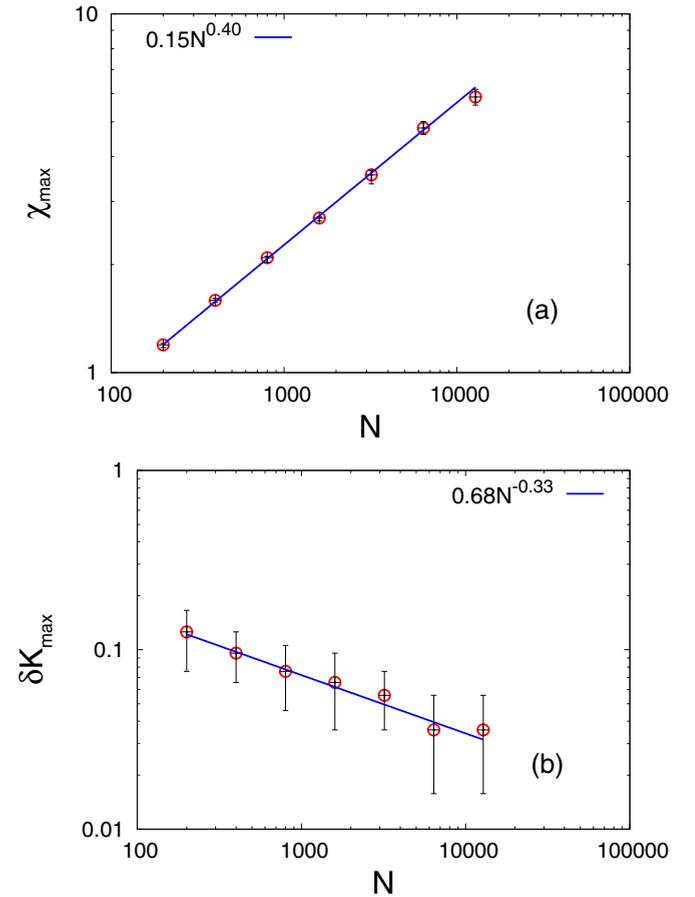

FIG. 2. (Color online) (a) Behavior of $\chi_{\max}$ is shown as a function of N in a log-log plot. The straight line obtained through the least-squares fitting method displays $\chi_{\max} \sim N^{0.40}$. (b) The behavior of $\delta K_{\max}$ ($= |K_{\max} - K_c|$) is shown as a function of N in a log-log plot. The straight line obtained through the least-squares fitting method displays $\delta K_{\max} \sim N^{-0.33}$.
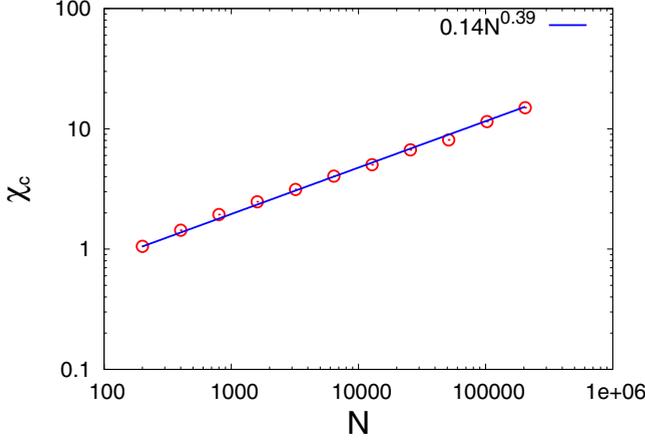
FIG. 3. (Color online) Critical increase of χ at K_c ($=\sqrt{8/\pi}$) is plotted as a function of N in a log-log plot. The slope of the straight line is 0.39. Statistical errors are represented by symbol sizes.

Even though our estimate of $1/\bar{\nu}'$ is rather weak due to huge statistical uncertainties in locating $K_{\max}$, it includes our analytic value of $1/\bar{\nu} = \frac{2}{5}$ within the error bar. Taking a simple ratio of the above exponent values, we estimate $\gamma' = 1.2(3)$. If we take $1/\bar{\nu}' = \frac{2}{5}$, then $\gamma' = 1.00(3)$.

We also measure the value of χ at the bulk critical point $K = K_c$. As K_c is located to the right of the peak position $K_{\max}(N)$ for all N in this case, the FSS behavior at K_c may be regarded as a continuation of the scaling on the supercritical side. Again, the FSS ansatz leads to

$$\chi_c \equiv \chi(\epsilon = 0, N) \sim N^{\gamma/\bar{\nu}}. \tag{3.12}$$

Figure 3 shows that the numerical data agree almost perfectly with the FSS ansatz with

$$\gamma/\bar{\nu} = 0.39(2). \tag{3.13}$$

This result confirms the ratio relation $\gamma/\bar{\nu} = \gamma'/\bar{\nu}'$, but it does not provide estimates for γ and $\bar{\nu}$ separately.

To estimate γ and γ' directly from off-critical data in Eq. (3.7), we examine the local slopes of χ against $|\epsilon|$ in double-logarithmic plots for very large N. The *effective exponent* γ_{eff} is defined as

$$\gamma_{\mathrm{eff}}(\epsilon) \equiv \frac{d \ln \chi}{d \ln |\epsilon|}, \tag{3.14}$$

and the critical exponents are obtained from their asymptotic values as $\gamma = \lim_{\epsilon \to 0^+} \gamma_{\mathrm{eff}}(\epsilon)$ and $\gamma' = \lim_{\epsilon \to 0^-} \gamma_{\mathrm{eff}}(\epsilon)$. Figure 4 shows the inverse of the effective exponent $\gamma_{\mathrm{eff}}^{-1}$ as a function of ϵ. We find that $\gamma_{\mathrm{eff}}^{-1}$ approaches γ'^{-1} linearly as ϵ goes to zero from below in the subcritical region, with its asymptotic value $\gamma' = 1.01(3)$. This is consistent with our previous numerical estimates and also with the theoretical prediction of $\gamma' = 1$ by Daido [4]. Note that $\gamma' = 1$ has also been obtained in a systematic $1/N$ expansion [5], where the random frequency distribution is a prerequisite.

On the supercritical side, $\gamma_{\mathrm{eff}}^{-1}$ varies in a nonlinear fashion far from the transition, but it approaches γ^{-1} linearly near small ϵ with the asymptotic value $\gamma = 0.98(5)$. This suggests strongly that $\gamma = \gamma' = 1$, and it definitely excludes Daido's
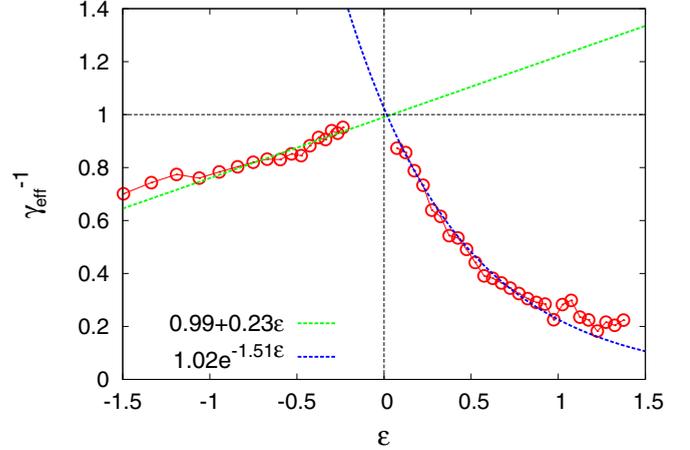

FIG. 4. (Color online) Numerical data for the inverse of the effective exponent $\gamma_{\mathrm{eff}}^{-1}$ are plotted against ϵ for $N = 12\,800$. Two dotted lines represent the fitting lines, indicating $\gamma \approx 0.98$ and $\gamma' \approx 1.01$.

value $\gamma = \frac{1}{4}$. With $\gamma = 1$, our numerical estimate in Eq. (3.13) leads to $\bar{\nu} = \bar{\nu}' = \frac{5}{2}$.

Summing up all these results, we conclude that our numerical data strongly support simple scaling exponents:

$$\beta = \frac{1}{2}, \quad \bar{\nu} = \bar{\nu}' = \frac{5}{2}, \quad \text{and} \quad \gamma = \gamma' = 1. \tag{3.15}$$

However, a proper analytic treatment for the dynamic fluctuations in the supercritical side is lacking, and further investigations are thus needed. One should note that the dynamic fluctuations of the order parameter are not necessarily proportional to the susceptibility (response of the order parameter to an infinitesimal external field) in general nonequilibrium steady states due to probable violation of the fluctuation-dissipation theorem. It is almost trivial to derive the susceptibility exponents in the Kuramoto model, which turn out to be $\gamma_{\mathrm{sus}} = \gamma'_{\mathrm{sus}} = 1$ [16]. Yet this accordance with the dynamic fluctuation exponents in Eq. (3.15) may be merely coincidental.

C. Hyperscaling relation

In the equilibrium critical phenomenon, the equation

$$\gamma = \bar{\nu} - 2\beta, \tag{3.16}$$

with $\bar{\nu} = d\nu$, is usually referred to as a hyperscaling relation. Here d is the dimension of the system and ν is the correlation length exponent. Equation (3.16) follows from a simple power counting of Eq. (3.6) at the transition. The left-hand side of Eq. (3.6) is $\chi_c \sim N^{\gamma/\bar{\nu}}$, while the right-hand side is proportional to $N^{1-2\beta/\bar{\nu}}$ if the leading-order terms do not exactly cancel each other out.

It is obvious that our result Eq. (3.15) does not satisfy this relation. Violating the hyperscaling relation is only possible when the leading-order terms in $[\langle \Delta^2 \rangle]$ and $[\langle \Delta \rangle^2]$ cancel out exactly, and the subleading-order terms show up, yielding $\gamma = 1$ instead of $\frac{3}{2}$. A plausible conjecture for leading and subleading terms for the large-N expansion of the two
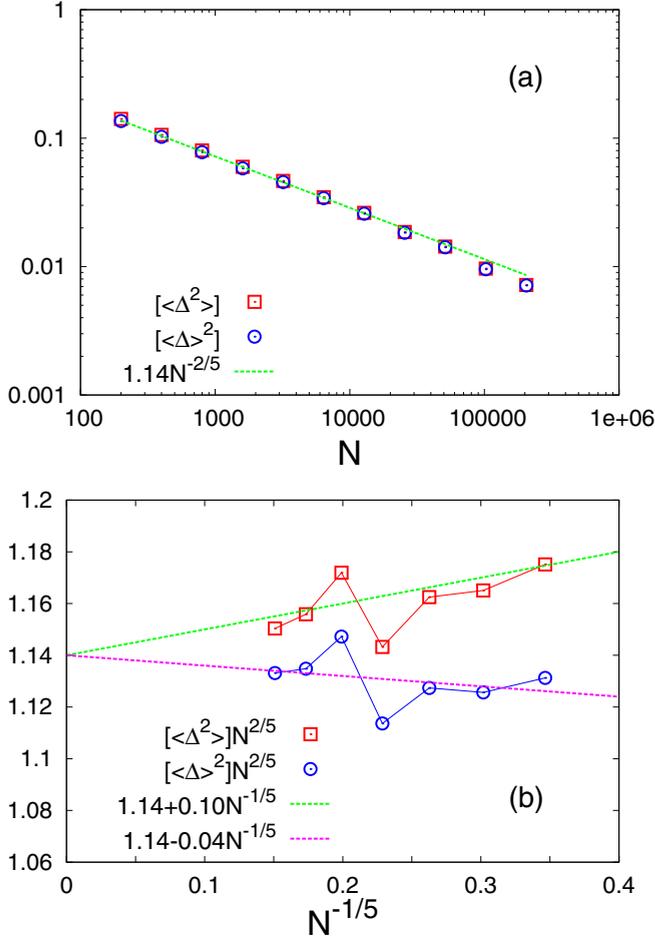
FIG. 5. (Color online) (a) Critical decay of $[\langle\Delta^2\rangle]$ and $[\langle\Delta\rangle^2]$ at K_c $(=\sqrt{8/\pi})$ is plotted against N in a log-log plot. These two data are so close to each other that it is not possible to discern two data in this plot. The straight line is the fitting line of $1.14N^{-0.40}$. (b) $N^{\frac{2}{5}}[\langle\Delta^2\rangle]$ and $N^{\frac{2}{5}}[\langle\Delta\rangle^2]$ vs $N^{-\frac{1}{5}}$. These data are expected to show straight lines. The least-squares fitting yields two straight lines with the same intercept. Lines between data are only guides to the eye.

quantities is then

$$[\langle\Delta^2\rangle] = N^{-2\beta/\bar{\nu}}\left(c + dN^{-\frac{1}{5}}\right),$$
$$[\langle\Delta\rangle^2] = N^{-2\beta/\bar{\nu}}\left(c' + eN^{-\frac{1}{5}}\right), \quad (3.17)$$

with $c = c'$. Indeed, our numerical data show in Fig. 5 that $c \approx c' = 1.140(2)$, $d = 0.10(4)$, and $e = -0.04(4)$. Then, the dynamic fluctuation χ at the transition scales as

$$\chi_c = (d - e)N^{1-2\beta/\bar{\nu}-\frac{1}{5}} \sim N^{\gamma/\bar{\nu}}, \quad (3.18)$$

yielding

$$\gamma = \bar{\nu} - 2\beta - \frac{1}{2} = 1. \quad (3.19)$$

The cancellation of the leading order ($c = c'$) in Eq. (3.17) would be expected if dynamic fluctuations only produce subleading order corrections to the solution of the mean-field equation (3.4) at the transition. Interestingly, as we show in Appendix, the mean-field approximation yields

$[\langle\Delta^2\rangle] = [\langle\Delta\rangle^2] \simeq 0.93N^{-\frac{2}{5}}$, which is smaller in amplitude as compared to the numerically determined value $c = 1.14$. Therefore, it appears that dynamic fluctuations renormalize the strength of the quenched noise $\delta\Psi$, but they do not change its scaling with N.

It is interesting to compare the violation of hyperscaling in the Kuramoto model to known cases in equilibrium phase transitions. One well-known such case is the incompatibility between the correlation length exponent $\nu = \frac{1}{2}$ at the Gaussian fixed point and the mean-field exponents $\beta = \frac{1}{2}$ and $\gamma = 1$ above the critical dimension $d_c = 4$ [17]. Violation of hyperscaling is also reported in the three-dimensional random-field Ising model, whose ordering transition is controlled by a zero-temperature fixed point [18–21]. In both cases, the energy associated with the symmetry-breaking field is much stronger than the thermal energy on large length scales, hence the order parameter fluctuations, as measured by the exponent γ, become less than what is predicted by the hyperscaling relation. In this sense, the weaker dynamic fluctuations of the order parameter in the Kuramoto model may be interpreted in a similar way, despite the fact that we are now in a nonequilibrium situation.

IV. REGULAR FREQUENCY DISTRIBUTION

In this section, we consider the "regular" frequency set $\{\omega_j\}$ with minimal disorder among frequencies. This set can be generated following a deterministic procedure given by

$$\frac{j - 0.5}{N} = \int_{-\infty}^{\omega_j} g(\omega)d\omega, \quad (4.1)$$

with $j = 1, \ldots, N$ and $g(\omega) = (1/\sqrt{2\pi})e^{-\omega^2/2}$. The generated frequencies are quasiuniformly spaced in accordance with $g(\omega)$ in the population. As this set is uniquely determined for each N, sample disorder may result from initial conditions only. Note that the regular frequency distribution is considered in numerical attempts by Daido [4].

Similar to the case of the random distribution, we numerically integrate Eq. (2.3) for system sizes up to $N = 12\,800$ with a discrete time step $\delta t = 0.01$, up to a total of 10^7 time steps. We start with random initial values of $\{\phi_j(0)\}$ and average the data over the latter half of the time steps, and we also average over 20–100 different samples of $\{\phi_j(0)\}$. At $K = K_c$, we perform numerical integration for larger systems up to $N = 25\,600$ with 10–100 samples.

A. Finite-size scaling of the order parameter

We measure the order parameter and its square during numerical integrations and average over time in the steady state, and then we average over samples with different initial values for the phase variables. These averages are denoted by $[\langle\Delta\rangle]$ and $[\langle\Delta^2\rangle]$, respectively. Figure 6 shows their size dependence at the transition ($\epsilon = 0$), exhibiting the nice power laws

$$[\langle\Delta\rangle] \sim N^{-0.39(2)} \quad \text{and} \quad [\langle\Delta^2\rangle] \sim N^{-0.78(3)}. \quad (4.2)$$
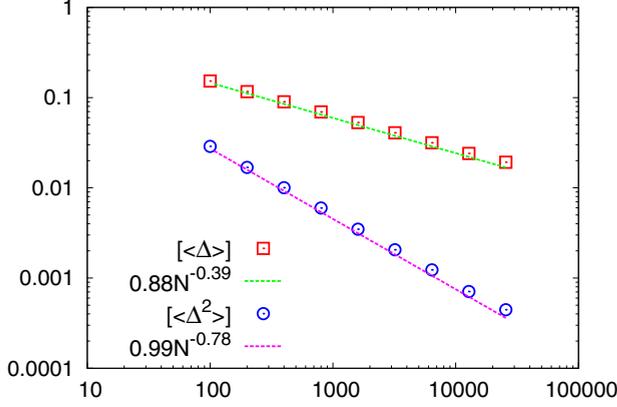
FIG. 6. (Color online) Critical decay of the order parameter [$\langle\Delta\rangle$] and [$\langle\Delta^2\rangle$] at K_c ($=\sqrt{8/\pi}$) is plotted as a function of N in a log-log plot, which are represented by (red) open boxes and (blue) open circles, respectively. The slopes of two straight lines are -0.39 and -0.78, respectively.

Following the FSS theory in Eqs. (3.1) and (3.2), we estimate the decay exponent as

$$\beta/\bar{\nu} = 0.39(2). \tag{4.3}$$

Given the value $\beta = \frac{1}{2}$, we obtain $\bar{\nu} \approx \frac{5}{4}$.

As a consistency check, we investigate the FSS relation in Eq. (3.1) for $\epsilon \neq 0$. We plot $\Delta N^{\beta/\bar{\nu}}$ versus $\epsilon N^{1/\bar{\nu}}$ for various system sizes N in Fig. 7. (For a moment, we drop the average brackets as $\Delta \equiv [\langle\Delta\rangle]$ for convenience). The data show a perfect collapse with the choice of $\bar{\nu} = \frac{5}{4}$. We also considered the regular Lorentzian distribution given by $g(\omega) = \gamma_\omega/[\pi(\omega^2 + \gamma_\omega^2)]$ with the half-width γ_ω, where the oscillator frequency is chosen as $\omega_j = \gamma_\omega \tan[j\pi/N - (N+1)\pi/(2N)]$ for $j = 1, \ldots, N$. We find a similar behavior again with $\bar{\nu} \approx \frac{5}{4}$.

B. Dynamic fluctuations

In this subsection, we present numerical data for the dynamic fluctuations χ in Fig. 8. Compared to the random distribution case, χ is very much reduced in magnitude and

FIG. 8. (Color online) Dynamic fluctuation χ is plotted as a function of ϵ ($=K - K_c$) for various system sizes N for the regular distribution, where $K_c = \sqrt{8/\pi}$. The solid (red) line represents a fitting line for data with the largest system size.

peaks only in a much narrower region around the transition. The small amplitude makes it difficult to determine the peak height and position accurately. However, with the exact information of $K_c = \sqrt{8/\pi}$, it is numerically feasible to investigate the critical increase of χ_c at the transition as a function of N. The data shown in Fig. 9 fit well to a power law

$$\chi_c \sim N^{\gamma/\bar{\nu}} \quad \text{with} \quad \gamma/\bar{\nu} = 0.22(2). \tag{4.4}$$

Using $\bar{\nu} = \frac{5}{4}$, we find $\gamma = 0.27(3)$, which is close to $\frac{1}{4}$. This value is consistent with Daido's theoretical result of $\gamma = \frac{1}{4}$ [4].

We also estimate γ and γ' directly from off-critical data by examining the effective exponents γ_{eff} for large N. Figure 10 shows $(4\gamma_{\text{eff}})^{-1}$ versus ϵ. Following a similar procedure as in the random case, we find $\gamma = 0.24(2)$ and $\gamma' = 0.25(1)$. We also fit the off-critical data directly in Fig. 8, which agree very well with $\chi \sim |\epsilon|^{-0.25}$. All the numerical results strongly
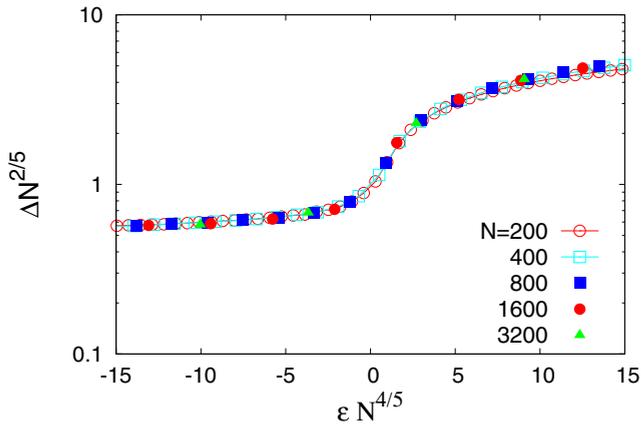

FIG. 7. (Color online) Scaling plot of the order parameter Δ for various system sizes N for the regular distribution. We use $\beta/\bar{\nu} = \frac{2}{5}$ and $\bar{\nu} = \frac{5}{4}$.
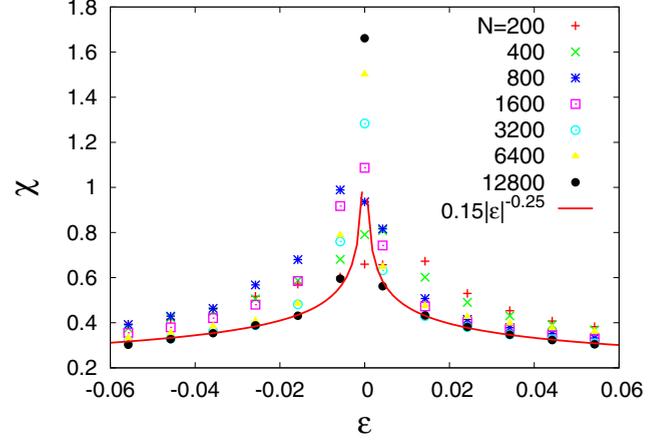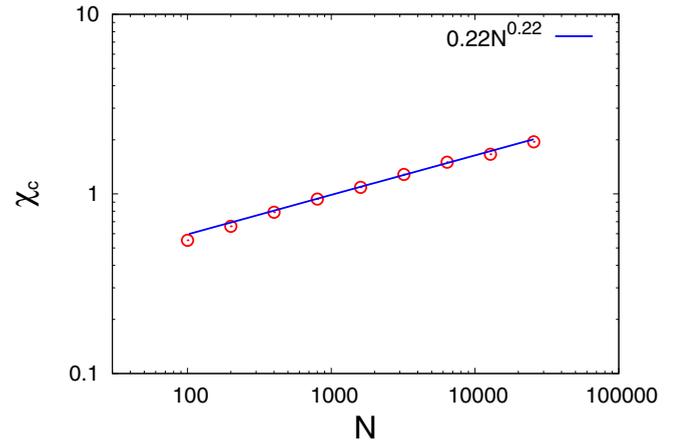

FIG. 9. (Color online) Critical increase of χ_c at K_c ($=\sqrt{8/\pi}$) is plotted as a function of N in a log-log plot for the regular distribution. The slope of the straight line is 0.22.
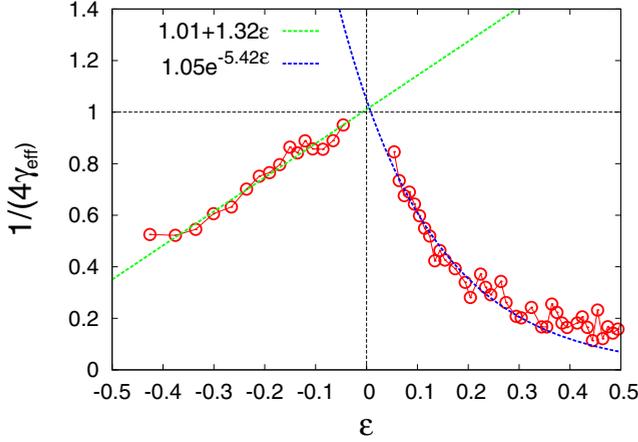
FIG. 10. (Color online) $1/(4\gamma_{\rm eff})$ vs ϵ for $N = 6400$. Two dotted lines represent the fitting lines, indicating $\gamma \approx 0.24$ and $\gamma' \approx 0.25$.

suggest scaling exponent values as

$$\beta = \tfrac{1}{2}, \quad \bar{\nu} = \bar{\nu}' = \tfrac{5}{4}, \quad \text{and} \quad \gamma = \gamma' = \tfrac{1}{4}. \quad (4.5)$$

Our results are clearly different from Daido's numerical suggestions of $\bar{\nu} \approx \tfrac{1}{2}$ and $\bar{\nu}' \approx 2$ and also his theoretical prediction of $\gamma' = 1$ on the subcritical side, which cannot be accounted for by adopting a slightly different definition of χ by Daido [15].

C. Hyperscaling relation

The hyperscaling relation, $\gamma = \bar{\nu} - 2\beta$, is seen to hold in the regular case. Furthermore, there is no detectable "disorder fluctuation" arising from different initial phase values, leading to $[\langle\Delta\rangle]^2 \approx [\langle\Delta\rangle^2]$.

V. SUMMARY

In this paper, we revisited the well-known Kuramoto model and investigated the FSS of the order parameter and its dynamic fluctuations near the onset of synchronization transition. We find that critical scaling behavior depends crucially on the presence of disorder among intrinsic frequencies of oscillators. In the random case with disorder, it is shown analytically and numerically that the FSS exponent $\bar{\nu} = \tfrac{5}{2}$ and the dynamic fluctuation exponent $\gamma \approx 1$, in both the supercritical and the subcritical region. In the regular case without disorder, we find $\bar{\nu} \approx \tfrac{5}{4}$ and $\gamma \approx \tfrac{1}{4}$. In both cases, the exponent $\bar{\nu}$ is different from its conventional value $\bar{\nu} = 2$ in usual mean-field theory of homogeneous systems with global coupling.

In the random case, disorder in the oscillator frequencies broadens the critical region and drives order parameter fluctuations in a sample-dependent manner. The hyperscaling relation that describes the interplay between static (i.e., averaged) and dynamic order parameter fluctuations is violated. Interestingly, a modified mean-field theory that completely ignores dynamic fluctuations yields correct critical FSS of the order parameter, although the amplitude is renormalized by dynamic fluctuations. This is one of the main findings in this work. In comparison, numerically determined exponents γ and $\bar{\nu}$ in the regular case satisfy the hyperscaling relation. Further

work is required to explain the particular values observed in our study.

APPENDIX: FINITE-SIZE SCALING IN THE MEAN-FIELD APPROXIMATION

In this Appendix, we consider in some detail the solution to the self-consistent mean-field equation (3.4). For this purpose, it is convenient to introduce a function

$$\psi(u) = \begin{cases} \sqrt{1 - u^2}, & |u| < 1, \\ 0, & |u| \geqslant 1. \end{cases} \quad (A1)$$

In terms of ψ, we have

$$\Psi(K\Delta) = \frac{1}{N} \sum_{j=1}^{N} \psi(\omega_j/K\Delta). \quad (A2)$$

Since each term in the sum is a monotonically increasing function of $z = K\Delta$, independent of the sign of ω_j, the sum is also a monotonically increasing function of z. In terms of z, Eq. (3.4) can be rewritten as

$$K^{-1}z = \Psi(z). \quad (A3)$$

When K is sufficiently small, only the trivial solution $z = 0$ is obtained. The nontrivial solution is obtained only for $K > K_c$, where K_c depends on the specific choice of the frequencies $\{\omega_j\}$.

We now consider the statistical properties of the solution to Eq. (A3) when the frequencies $\{\omega_j\}$ are drawn independently from a given distribution $g(\omega)$. In this case, $\psi_j \equiv \psi(\omega_j/z)$ are also independent random variables whose distribution can be obtained from $g(\omega)$. The quantity Ψ as defined by Eq. (A2) is simply the average of the random variables ψ_j, $j = 1, \ldots, N$. Its mean value is given by $[\psi]$. Let $\delta\Psi = \Psi - [\psi]$. Its variance is given by

$$[(\delta\Psi)^2] = \frac{[\psi^2] - [\psi]^2}{N}. \quad (A4)$$

The variance of ψ can be easily computed from $g(\omega)$:

$$\begin{aligned}
[\psi^2] - [\psi]^2 &= \int_{-z}^{z} d\omega \, g(\omega) \left[1 - \left(\frac{\omega}{z} \right)^2 \right] \\
&\quad - \left[\int_{-z}^{z} d\omega \, g(\omega) \sqrt{1 - \left(\frac{\omega}{z} \right)^2} \right]^2 \\
&= \frac{4}{3} g(0) z - \left(\frac{\pi}{2} g(0) \right)^2 z^2 + \cdots. \quad (A5)
\end{aligned}$$

Invoking the central limit theorem, we conclude that the distribution of Ψ tends to a Gaussian at large N, with mean and variance as stated above.

For small z,

$$[\psi] = \int_{-z}^{z} d\omega\, g(\omega)\sqrt{1 - \left(\frac{\omega}{z}\right)^2}$$

$$= \frac{\pi}{2}g(0)z + \frac{\pi}{16}g''(0)z^3 + \cdots. \qquad (A6)$$

Equation (A3) can now be written in the form

$$K^{-1}z = K_c^{-1}z - cz^3 + d\left(\frac{z}{N}\right)^{\frac{1}{2}}\eta, \qquad (A7)$$

where $K_c^{-1} = \pi g(0)/2$, $c = -\pi g''(0)/16 > 0$, and $d = [4g(0)/3]^{\frac{1}{2}}$. Here $\eta = \delta\Psi/[\delta\Psi^2]^{\frac{1}{2}}$ is a Gaussian random variable with zero mean and unit variance.

Solution to Eq. (A7) can be cast in the scaling form (3.1) with $\beta = \frac{1}{2}$ and $\bar{\nu} = \frac{5}{2}$. Specifically, let $z = K_c N^{-\frac{1}{5}}f$, Eq. (A7) becomes

$$xf - cK_c^3 f^3 + \left(\frac{8}{3\pi}\right)^{\frac{1}{2}}f^{\frac{1}{2}}\eta = 0, \qquad (A8)$$

where $x = N^{\frac{2}{5}}(K - K_c)/K$ is the scaled distance to the transition point.

We now consider a solution to Eq. (A8) at $K = K_c$ or $x = 0$. Simple algebra yields

$$f(0) = \begin{cases} A\eta^{\frac{2}{5}}, & \eta > 0, \\ 0, & \eta \leqslant 0. \end{cases} \qquad (A9)$$

Here $A = (8/3\pi)^{\frac{1}{5}}c^{-\frac{2}{5}}K_c^{-\frac{6}{5}}$. The nth moment of $f(0)$ at the transition is given by ($n > 0$),

$$[f^n(0)] = \frac{1}{(2\pi)^{\frac{1}{2}}}\int_0^{\infty} d\eta\, e^{-\eta^2/2}A^n\eta^{2n/5}$$

$$= \frac{A^n}{(2\pi)^{\frac{1}{2}}}\int_0^{\infty} dt\, e^{-t}(2t)^{n/5-\frac{1}{2}}$$

$$= \frac{2^{n/5}}{2\pi^{\frac{1}{2}}}A^n\Gamma\left(\frac{n}{5} + \frac{1}{2}\right). \qquad (A10)$$

In the special case $g(\omega) = e^{-\omega^2/2}/\sqrt{2\pi}$, $A = (8\pi/3)^{\frac{1}{5}}$. The first four moments are then given by

$$[f(0)] = \frac{1}{2\pi^{\frac{1}{2}}}\left(\frac{16\pi}{3}\right)^{\frac{1}{5}}\Gamma\left(\frac{7}{10}\right) = 0.643\,454\ldots,$$

$$[f^2(0)] = \frac{1}{2\pi^{\frac{1}{2}}}\left(\frac{16\pi}{3}\right)^{\frac{2}{5}}\Gamma\left(\frac{9}{10}\right) = 0.930\,853\ldots,$$

$$[f^3(0)] = \frac{1}{2\pi^{\frac{1}{2}}}\left(\frac{16\pi}{3}\right)^{\frac{3}{5}}\Gamma\left(\frac{11}{10}\right) = 1.456\,21\ldots,$$

$$[f^4(0)] = \frac{1}{2\pi^{\frac{1}{2}}}\left(\frac{16\pi}{3}\right)^{\frac{4}{5}}\Gamma\left(\frac{13}{10}\right) = 2.413\,98\ldots.$$

[1] A. T. Winfree, J. Theor. Biol. **16**, 15 (1967); Y. Kuramoto, in *Proceedings of the International Symposium on Mathematical Problems in Theoretical Physics*, edited by H. Araki (Springer-Verlag, New York, 1975); A. T. Winfree, *The Geometry of Biological Time* (Springer, New York, 1980); Y. Kuramoto, *Chemical Oscillations, Waves, and Turbulence* (Springer, Berlin, 1984); Y. Kuramoto and I. Nishikawa, J. Stat. Phys. **49**, 569 (1987).

[2] S. H. Strogatz, Physica D **143**, 1 (2000); A. S. Pikovsky, M. Rosenblum, and J. Kurths, *Synchronization: A Universal Concept in Nonlinear Science* (Cambridge University Press, Cambridge, 2001).

[3] For a recent review, see J. A. Acebrón, L. L. Bonilla, C. J. P. Vicente, and R. Spigler, Rev. Mod. Phys. **77**, 137 (2005), and references therein.

[4] H. Daido, Prog. Theor. Phys. **75**, 1460 (1986); J. Phys. A **20**, L629 (1987); Prog. Theor. Phys. **81**, 727 (1989); J. Stat. Phys. **60**, 753 (1990).

[5] E. J. Hildebrand, M. A. Buice, and C. C. Chow, Phys. Rev. Lett. **98**, 054101 (2007); M. A. Buice and C. C. Chow, Phys. Rev. E **76**, 031118 (2007).

[6] I. Z. Kiss, Y. Zhai, and J. L. Hudson, Science **296**, 1676 (2002); Phys. Rev. Lett. **94**, 248301 (2005).

[7] H. Hong, H. Park, and M. Y. Choi, Phys. Rev. E **72**, 036217 (2005).

[8] H. Hong, H. Chaté, H. Park, and L.-H. Tang, Phys. Rev. Lett. **99**, 184101 (2007).

[9] H. Hong, H. Park, and L.-H. Tang, Phys. Rev. E **76**, 066104 (2007).

[10] L.-H. Tang, J. Stat. Mech. (2011) P01034.

[11] H. Hong, J. Um, and H. Park, Phys. Rev. E **87**, 042105 (2013).

[12] S. H. Strogatz and R. E. Mirollo, J. Phys. A **21**, L699 (1988); **21**, 4649 (1988); Physica D **31**, 143 (1988).

[13] See e.g., R. L. Burden and J. D. Faires, *Numerical Analysis* (Brooks/Cole, Pacific Grove, 1997), p. 280.

[14] J. Um, H. Hong, and H. Park, Phys. Rev. E **89**, 012810 (2014).

[15] In Ref. [4], a slightly different definition for dynamic fluctuations is adopted as $N[\langle|Z|^2\rangle - |\langle Z\rangle|^2]$ with the complex order parameter Z in Eq. (2.2). Given that the dynamic equations (2.1) have the symmetry of $\phi_j \to \phi_j + \text{const}$ for all j, this quantity behaves in the same way as $N[\langle\Delta^2\rangle]$ in the absence of symmetry breaking, which is expected of a finite system.

[16] H. Daido, Phys. Rev. E **91**, 012925 (2015).

[17] H. Hong, M. Ha, and H. Park, Phys. Rev. Lett. **98**, 258701 (2007); E. Brézin, J. Phys. (Paris) **43**, 15 (1982); K. Binder, M. Nauenberg, V. Privman, and A. P. Young, Phys. Rev. B **31**, 1498 (1985).

[18] J. Villain, J. Phys. (France) **46**, 1843 (1985).

[19] D. S. Fisher, Phys. Rev. Lett. **56**, 416 (1986); A. A. Middleton and D. S. Fisher, Phys. Rev. B **65**, 134411 (2002).

[20] T. Nattermann, in *Spin Glasses and Random Fields*, edited by A. P. Young (World Scientific, Singapore, 1998), p. 277.

[21] R. L. C. Vink, T. Fischer, and K. Binder, Phys. Rev. E **82**, 051134 (2010).